J Solid State Electrochem (2003) 7: 492–496
DOI 10.1007/s10008-003-0375-y

ORIGINAL PAPER

S. S. Zhang · K. Xu · T. R. Jow

Alkaline composite film as a separator for rechargeable lithium batteries

Received: 2 December 2002 / Accepted: 7 February 2003 / Published online: 21 May 2003

Abstract We report a new type of separator film for application in rechargeable lithium and lithium-ion batteries. The films are made of mainly alkaline calcium carbonate ($CaCO_3$) and a small amount of polymer binder. Owing to porosity and capillarity, the composite films show excellent wettability with non-aqueous liquid electrolytes. Typically, the composite films composed of $CaCO_3$ and Teflon and wetted with 1 M $LiPF_6$ dissolved in a solvent mixture of ethylene carbonate (EC) and ethyl methyl carbonate (EMC) (30:70 wt%) exhibit an ionic conductivity as high as 2.5–4 mS/cm at 20 °C, in a comparable range with that (3.4 mS/cm) of the commercial Celgard membrane. In the batteries, the composite film not only serves as a physical separator but also neutralizes acidic products, such as HF formed by $LiPF_6$ hydrolysis, as well as those formed by solvent oxidative decomposition. A $Li/LiMn_2O_4$ test cell was employed to examine the electrochemical compatibility of the composite film. We observed that the composite film cell showed an improved cycling performance since the alkaline $CaCO_3$ neutralizes the acidic products, which otherwise promote dissolution of the electrode active materials. More importantly, the composite film cell displayed a superior performance on high-rate cycling, which was probably the result of the less resistive interface formed between the electrode and the composite film.

Keywords Composite film · High-rate performance · Ionic conductivity · Lithium-ion battery · Separator

Introduction

A microporous polypropylene (Celgard) membrane has been used as a physical separator between cathode and anode in commercial lithium-ion batteries. It is well known that polypropylene materials start softening and melting above 130 °C, depending on their average molecular weight, which is a temperature easily achieved under abuse conditions such as short circuiting and overcharge [1, 2, 3]. Owing to softening, melting and its resulting volume shrinkage, the polymeric membrane fails as a separator for the cathode and anode, which may cause internal short circuiting or, worse, lead to a catastrophic thermal runaway. In addition, the Celgard membrane cannot withstand penetration of the dendrite metal lithium formed during charging. Therefore, it is necessary to develop an alternative separator, which not only is mechanically strong but also is dimensionally stable at elevated temperatures. For this purpose, we have fabricated a porous composite film with its major constituent being a rigid inorganic material.

$LiPF_6$ has been the only choice for the electrolyte solute in the state-of-the-art lithium-ion batteries owing to its advantages such as providing high ionic conductivity [4], being able to passivate the aluminum current collector of the cathode [5], and favoring formation of a solid electrolyte interface (SEI) on the surface of a graphite electrode [6]. Unfortunately, $LiPF_6$ is highly sensitive to moisture and is thermally unstable [7]. It has been proven that $LiPF_6$ is one of the major causes for capacity fading of lithium-ion batteries since its hydrolysis produces acidic HF. This HF subsequently promotes dissolution of the cathode active materials, especially the spinel $LiMn_2O_4$ [8, 9]. Considering the above facts, we have employed alkaline $CaCO_3$ as the major constituent of the separator film and to explore the additional benefits of this composite film. In this work, a $Li/LiMn_2O_4$ button cell was used to evaluate the electrochemical compatibility of the composite films. Although our goal is to coat directly the separator film onto the electrode surface, in this work we have intentionally fabricated a self-standing film for the purpose of convenient measurement of the geometric dimensions and the ionic conductivity of the films. In this paper we will discuss the ionic conductivity of the electrolyte-wetted films and explore their application in lithium-ion

S. S. Zhang (✉) · K. Xu · T. R. Jow
Army Research Laboratory,
Adelphi, MD, 20783, USA

batteries by using the $Li/LiMn_2O_4$ cell as the testing vehicle.

Experimental

Spinel $Li_xMn_2O_4$ ($x=1.0$, EM Industries) and $CaCO_3$ (10 μm, 98%, Aldrich) were respectively pressed to form a flexible self-standing film by using a Teflon (emulsion, Du Pont) binder, as described elsewhere [10]. The cathode film was composed of 80% $LiMn_2O_4$, 19% acetylene black (Alfa), and 1% Teflon (by weight), and the composite film of 92% $CaCO_3$ and 8% Teflon unless specified otherwise. Both cathode and separator films were dried at 120 °C under vacuum for 16 h before use. The liquid electrolyte used was a solution prepared by dissolving 1.0 M $LiPF_6$ (Stella Chemica) in a solvent mixture of ethylene carbonate (EC, Grant Chemical) and ethyl methyl carbonate (EMC, Grant Chemical) in a 3:7 weight ratio. The water content of the electrolyte as determined by Karl-Fisher titration was 10–15 ppm. In an argon-filled glove box, $Li/LiMn_2O_4$ button cells with an electrode area of 1.27 cm^2 were assembled and filled with 150 μL of liquid electrolyte by using the commercial Celgard 2500 membrane and composite film, respectively, as the separator. The same button cells with stainless steel electrodes replacing Li and $LiMn_2O_4$ were assembled to measure the ionic conductivity of the separator films.

A Tenney environmental oven (series 942) was used to provide a constant temperature environment for the tests at various temperatures. A Solartron SI 1287 electrochemical interface and a SI 1260 impedance/gain-phase analyzer were adopted for the measurements of impedance and cyclic voltammetry. The obtained data were analyzed using either ZView or CorrView software (Scribner). Charge–discharge cycling tests of the cells were carried out on a Maccor series 4000. For testing of the rate performance, we charged the cells at 0.5 mA and discharged at a specific current as described in the text.

Results and discussion

Ionic conductivity of the electrolyte-wetted composite film

The Teflon-bonded composite films are porous, flexible, and self-standing. We found that the liquid electrolytes can rapidly spread throughout the resultant composite films owing to the porosity of the film and the capillarity of the particle surface. Therefore, ionic conductivity of the composite films can be easily achieved by simple take-up of an appropriate amount of liquid electrolyte. Figure 1 shows the ionic conductivity of the electrolyte-wetted composite films. For the purpose of comparison, the conductivities of the liquid electrolyte and the commercial Celgard 2500 membrane wetted with the same liquid electrolyte are also plotted in Fig. 1. In both of the above membranes, the liquid electrolytes are believed to distribute in the pores between either the inert polypropylene host or the $CaCO_3$ particles. Therefore, it may be considered that the ionic conductivities of the above electrolyte-wetted films completely originate from a contribution of the absorbed liquid electrolyte. It is shown in Fig. 1 that the composite films wetted with the liquid electrolyte show a similar ionic conductivity as the Celgard membrane. For example, at 20 °C the ionic conductivities of the composite films are in the range

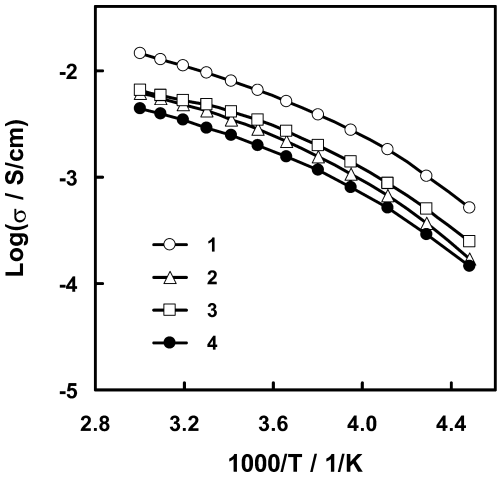

Fig. 1 Arrhenius plots of the ionic conductivities for the liquid electrolyte and its wetted separators: (*1*) liquid electrolyte; (*2*) Celgard membrane; (*3*) composite film of $CaCO_3$ and Teflon (98:2 wt%); and (*4*) composite film of $CaCO_3$ and Teflon (92:8 wt%)

2.5–4 mS/cm versus 3.4 mS/cm for the Celgard membrane. We noticed that the ionic conductivity of the composite films is significantly increased on decreasing the content of the Telfon binder. Assuming that the ionic conductivity of the composite film is affected by only the volumetric fraction of the liquid electrolyte in the film, one may estimate the effective porosity (P) of the composite films by the equation:

$$P = \frac{\sigma_{\text{film}}}{\sigma_{\text{liquid}}} \tag{1}$$

where σ_{film} and σ_{liquid} are the ionic conductivities of the composite film and the pure liquid electrolyte, respectively. According to Eq. 1, the effective porosity of a $CaCO_3$/Teflon (92:8 wt%) film is determined to be 30%. We believe that the actual (physical) porosity must be higher than the effective porosity since the liquid electrolyte cannot completely penetrate into all the pores. An important feature of the composite films is that their wettability is scarcely affected by the electrolyte solvents. Therefore, such films can be coupled with all non-aqueous liquid electrolytes without any problem of wettability, which certainly facilitates the process of electrolyte filling in the battery assembly.

Impedance of the $Li/LiMn_2O_4$ cells with the composite film

In earlier work [11], we have found that impedance of the $Li/LiMn_2O_4$ cells greatly varies with the cell voltage owing to the high sensitivity of the cathode volume and charge-transfer kinetics to the state-of-charge (SOC). For a fair comparison, we therefore selected a fully charged state (SOC = 100%) to analyze the impedance of the cells. Figure 2 compares Nyquist plots of two fully charged $Li/LiMn_2O_4$ cells, one using a Celgard mem-

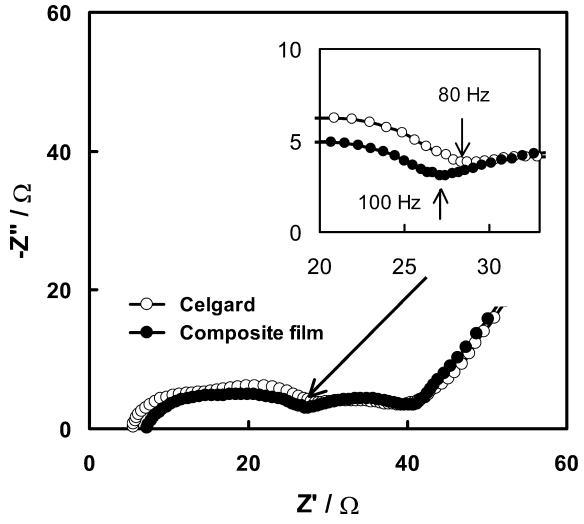

Fig. 2 Nyquist plots of the $Li/LiMn_2O_4$ cells, which were recorded at 4.2 V and at 20 °C

brane and the other the composite film, which were potentiostatically measured at 4.2 V. The impedance spectra in Fig. 2 can be explained using an equivalent circuit comprising a series of combinations of the resistance and capacitance [11, 12]. The intercept at the high-frequency end reflects the bulk resistance (R_b) of the electrodes and separator (wetted with the electrolyte). The two overlapped semicircles in the medium-frequency regions, which are often merged into a single semicircle in many cases, reflect the resistance (R_{sl}) and relative capacitance of the complicated interphase layer between the electrode and separator. The semicircle in the low-frequency regions corresponds to the charge-transfer resistance (R_{ct}) and double-layer capacitance of the faradic reactions taking place in the interface between the electrode and separator. The straight sloping line at the low-frequency end is related to the diffusion of lithium ions in the bulk of the electrodes and separator. It is estimated from Fig. 2 that R_b is 5.6 Ω and 7.4 Ω for the Celgard membrane cell and composite film cell, respectively. A slightly larger R_b for the composite cell is not only because the composite film has lower ionic conductivity (Fig. 1), but also because it has a higher thickness than the Celgard membrane. However, the composite film cell exhibits a lower R_{sl} (see inset in Fig. 2) so that the total impedances of these two cells are almost the same. Furthermore, the frequency at the cross of the R_{sl} and R_{ct} semicircles for the composite film cell is slightly higher, i.e. 100 Hz versus 80 Hz, as shown in the inset of Fig. 2. The above results indicate that the composite film forms a less resistive separator/electrode interface layer.

Electrochemical compatibility of the composite film

While introducing a material with small particle size into the batteries, one must consider its catalytic effect on the electrochemical decomposition of the electrolyte solvents. Therefore, we used cyclic voltammetry and galvanostatic cycling tests to evaluate the electrochemical compatibility of the composite film. Cyclic voltammograms of the Celgard membrane cell and the composite film cell are both plotted in Fig. 3. The cyclic voltammogram of the $Li/LiMn_2O_4$ cells is composed of two pairs of well-separated current peaks. It is known [13] that these two pairs of current peaks correspond to a two-step phase transitions of the spinel $LiMn_2O_4$, i.e. λ-$MnO_2 \leftrightarrow Li_{0.5}Mn_2O_4$ and $Li_{0.5}Mn_2O_4 \leftrightarrow LiMn_2O_4$. It is calculated from the cyclic voltammograms that the specific capacities of the spinel $LiMn_2O_4$ are 105 mA h/g and 110 mA h/g in the composite film cell and Celgard cell, respectively, and that both cells have the same coulomb efficiency of 95%. As shown in Fig. 3, cyclic voltammograms of these two cells nearly overlap, and the anodic currents decrease to the background as the voltage is increased to 4.3 V. These results verify that the electrolyte solvent is electrochemically stable with the composite film.

Figure 4 plots voltage profiles for the charge and discharge cycling of the $Li/LiMn_2O_4$ cells. The specific capacity and coulomb efficiency of the spinel $LiMn_2O_4$ with the composite film separator, as obtained from the galvanostatic cycling test, are respectively 116 mA h/g and nearly 100%, which are somewhat higher than those obtained from the cyclic voltammetry result. As Fig. 4 shows, there are two voltage plateaus in the voltage profiles of the charge and discharge processes, which can be more distinctly displayed in a differential capacity–voltage plot (see inset in Fig. 4). A sharp increase of the cell voltage in the charging end (near 4.3 V) further verifies that the composite film is electrochemically compatible with the electrolyte solvents.

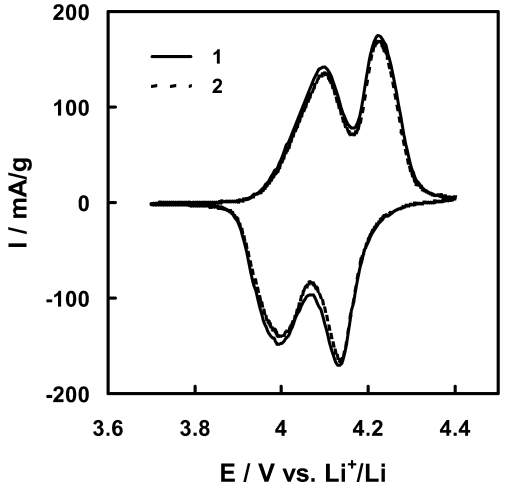

Fig. 3 Cyclic voltammograms of the $Li/LiMn_2O_4$ cells, which were recorded at 0.1 mV/s from the second cycle: (*1*) Celgard membrane and (*2*) the composite film

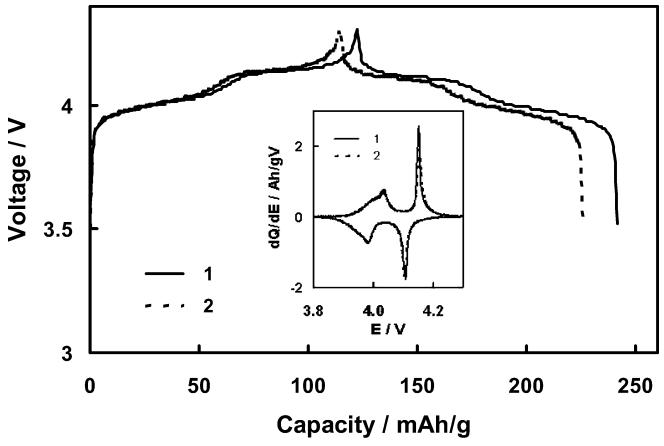

Fig. 4 Voltage–capacity profiles of the charge and discharge processes for the $Li/LiMn_2O_4$ cells, which were recorded at 0.3 mA/cm^2: (*1*) Celgard membrane and (*2*) the composite film

Cycling performance of the $Li/LiMn_2O_4$ cell using the composite film

Discharge capacities of the $Li/LiMn_2O_4$ cells are plotted as a function of the cycle number in Fig. 5. It is observed that the Celgard membrane cell and the composite film cell had similar capacities in the initial cycles. The capacities gradually decreased with the cycle number. After many cycles, however, the composite film cell maintained slightly higher capacities. It has been reported [14, 15] that spinel structural degradation and active material dissolution are two key sources for the capacity fading of the $LiMn_2O_4$ spinel. Of these two sources, the active material dissolution is known to be closely associated with the presence of acidic products, which are often formed during $LiPF_6$ hydrolysis and solvent oxidizing decomposition [15, 16]. Therefore, removal of these acid products would be expected to improve the cycling performance of the $LiMn_2O_4$ spinel. We consider that the alkaline $CaCO_3$ can neutralize the formed acids by the reaction:

$$2H^+ + 2CaCO_3 \rightarrow Ca(HCO_3)_2 + Ca^{2+} \quad (2)$$

Therefore, the observed improvement in Fig. 5 can be ascribed to the ability of the alkaline $CaCO_3$-based composite film in neutralizing acidic products present in the liquid electrolyte.

High-rate cycling performance of the $Li/LiMn_2O_4$ cell

The effect of the separators on the rate performance of the $Li/LiMn_2O_4$ cells is displayed in Fig. 6, in which the two cells had the same electrode area (1.27 cm^2) and capacity (1.1 mA h, as obtained at 0.5 mA between 3.5 V and 4.2 V). In these experiments the cells were run for two cycles at each current rate and an averaged capacity was used to calculate the relative capacity, which is defined as the percentage of the discharge capacity at a specific current to the capacity obtained at 0.5 mA. It is observed that the composite film cell retained at least the same or even better relative capacities compared to the Celgard membrane cell, although its R_b value is relatively higher (see Fig. 2). As discussed above, this surprising phenomenon can be ascribed to the formation of a less resistive interface layer between the electrode and separator. It is important to note that the composite film cell maintains higher capacities for currents higher than 6 mA (5.5 C rate).

Voltage–capacity profiles of the composite film cell at various discharge currents are plotted in Fig. 7. It is shown that both the capacity and operating voltage of the cell decreased with increase of the discharge current. This can be explained in the terms of *IR* polarization, which increases with the discharge current. Figure 7 shows that the two voltage plateaus disappear when the current reaches or exceeds 7.0 mA. In these cases, we noticed that the discharge processes were terminated by the pre-set voltage limit (3.5 V) rather than by the rapid drop in the discharge voltage, which is a common observation of the discharge end as observed from the discharge at lower currents. Considering this factor, we

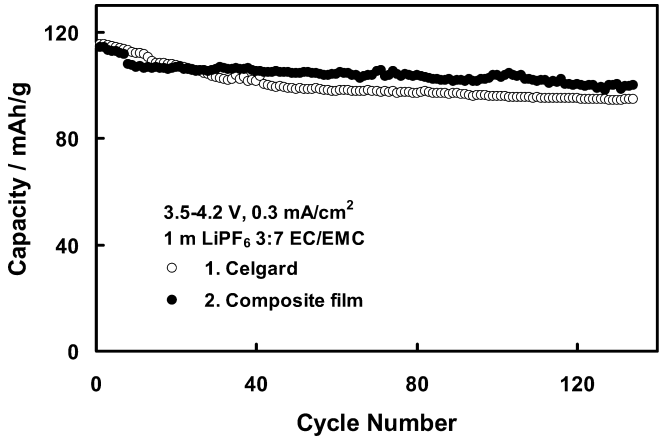

Fig. 5 Discharge capacities as a function of the cycle number for the $Li/LiMn_2O_4$ cells

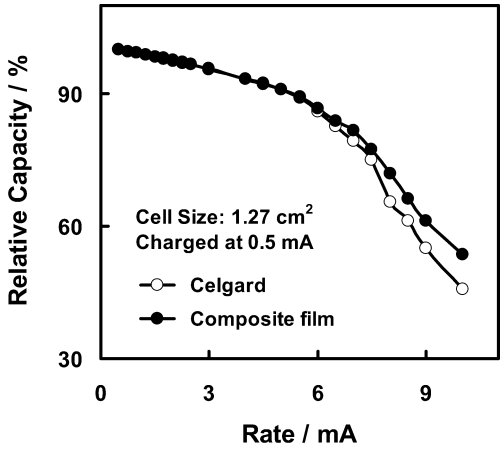

Fig. 6 Plots of the relative capacities versus discharge current for the $Li/LiMn_2O_4$ cells

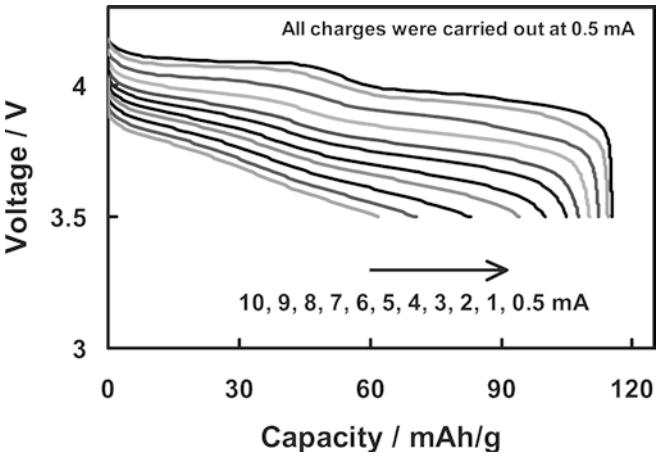

Fig. 7 Voltage–capacity profiles of the discharge process for the composite film $Li/LiMn_2O_4$ cell, in which the numbers show the current used in the discharge process

believe that the actual relative capacities at currents of more than 7.0 mA would be higher than those plotted in Fig. 6.

Conclusion

The alkaline $CaCO_3$-based composite films not only are wettable by non-aqueous liquid electrolytes, but also are electrochemically compatible with the electrolyte solvents. Wetted with a liquid electrolyte (1 M $LiPF_6$ dissolved in a solvent mixture of EC and EMC in 3:7 weight ratio), the composite films can provide an ionic conductivity (2–4 mS/cm at 20 °C) comparable to the commercial Celgard membrane. The advantages of the composite films include thermally dimensional stability, excellent wettability with the liquid electrolytes, and the ability to neutralize the acidic products. Furthermore, a less resistive interface can be formed between the composite film and the electrode. Its alkaline property can result in an improved cycling performance for $Li/LiMn_2O_4$ cells. The formation of a less resistive interface layer between the electrode and separator helps to improve the high-rate cycling performance.

References

1. Pasquier AD, Disma F, Bowmer T, Gozdz AS, Amatucci G, Tarascon JM (1999) J Electrochem Soc 145:472
2. Hong JS, Maleki H, Hallaj SA, Redey L, Selman JR (1998) J Electrochem Soc 145:1489
3. Maleki H, Hallaj SA, Selman JR, Dinwiddie RB, Wang H (1999) J Electrochem Soc 146:947
4. Ding MS, Xu K, Zhang SS, Jow TR, Amine K, Henriksen GL (2001) J Electrochem Soc 148:A1196
5. Zhang SS, Jow TR (2002) J Power Sources 109:458
6. Takami N, Ohsaki T, Inada K (1992) J Electrochem Soc 139:1849
7. Aldrich (2002) Lithium hexafluorophosphate material safety data sheet. Aldrich, Milwaukee, Wisc., cat. no. 2132440-3
8. Xia Y, Zhou Y, Yoshio M (1997) J Electrochem Soc 144:2593
9. Jang DH, Shin YJ, Oh SM (1996) J Electrochem Soc 143:2204
10. Zhang SS, Jow TR (2002) J Power Sources 109:173
11. Zhang SS, Xu K, Jow TR (2002) J Electrochem Soc 149:A1521
12. Zhang SS, Xu K, Allen JL, Jow TR (2002) J Power Sources 110:216
13. Liu W, Farrington GC, Chaput F, Dunn B (1996) J Electrochem Soc 143:879
14. Premanand R, Durairajan A, Haran B, White R, Popov BN (2002) J Electrochem Soc 149:A54
15. Ramadass P, Haran B, White R, Popov BN (2002) J Power Sources 111:210
16. Wang E, Ofer D, Bowden W, Iltchev N, Moses R, Brandt K (2000) J Electrochem Soc 147:4023